Contrib Mineral Petrol (2003) 146: 28–43
DOI 10.1007/s00410-003-0490-x

ORIGINAL PAPER

Bernardo Cesare · Maria Teresa Gómez-Pugnaire
Daniela Rubatto

Residence time of S-type anatectic magmas beneath the Neogene Volcanic Province of SE Spain: a zircon and monazite SHRIMP study

Received: 7 August 2002 / Accepted: 3 June 2003 / Published online: 26 July 2003

Abstract Zircon and monazite from three restitic enclaves and one host dacite have been dated by ion microprobe (SHRIMP), with the aim of characterising their Miocene history and defining the timing relationships between crustal melting and eruption in the high-K calc-alkaline volcanics of the Neogene Volcanic Province of SE Spain. The studied samples are from the volcanic edifices of El Joyazo (Cerro del Hoyazo) and Mazarrón. Zircons in the enclaves are characterized by a thin euhedral rim overgrowing a detrital core. The core-rim boundary is marked by tiny glass inclusions of S-type granitic composition, which attest to the growth of zircon rims during a crustal melting event. At El Joyazo, where lavas erupted at 6.3 Ma (Zeck and Williams 2002), U-Pb ages of zircon overgrowths define an age of anatexis of 9.63 ± 0.26 Ma (95% c.l.), in agreement with monazite ages of 9.74 ± 0.21 Ma (95% c.l.). At Mazarrón, the age of anatexis provided by monazite at 9.13 ± 0.18 Ma (95% c.l.) overlaps with that of melt-precipitated zircon in the host dacite, dated at 9.06 ± 0.53 Ma (95% c.l.). These results indicate that after partial melting, the enclaves and the syngenetic S-type melts resided at depth for >3 m.y. at El Joyazo. Compared with the results from Mazarrón, the long residence time obtained at El Joyazo is probably due to the greater depth of melting (c. 25 km vs. c. 15 km). At such depth, corresponding to the Miocene palaeo-Moho, the more ductile regime of the crust is likely to have favoured magma ponding. The thermal anomaly beneath the Neogene Volcanic Province, which generated the S-type crustal melts, is today visible from geophysical data and can be traced back to the Lower Miocene. As a consequence, residence times longer than determined in this work may be expected.

B. Cesare (✉)
Dipartimento di Mineralogia e Petrologia,
Università di Padova, Corso Garibaldi 37,
35137 Padova, Italy
E-mail: bernardo.cesare@unipd.it
Tel.: +39-49-8272019
Fax: +39-49-8272010

B. Cesare
C.N.R. Istituto di Geoscienze e Georisorse,
Corso Garibaldi 37, 35137 Padova, Italy

M. T. Gómez-Pugnaire
Departamento de Mineralogía y Petrología,
Facultad de Ciencias, Universidad de Granada,
Fuentenueva s/n, 18002 Granada, Spain

D. Rubatto
Research School of Earth Sciences,
Australian National University,
ACT 0200, Canberra, Australia

Present address: D. Rubatto
Department of Geology, Australian National University,
ACT 0200 Canberra , Australia

Editorial responsibility: J. Hoefs

Introduction

Partial melting is a key process linking metamorphism and magmatism, and plays a key role in the development of migmatites, granulites and S-type granites during crustal evolution. A possible geodynamic setting for partial melting of the middle and upper continental crust is extensional plate margins, where intense and prolonged positive thermal anomalies are developed by the uprise of hot asthenosphere or by the emplacement of mantle-derived magmas.

The Internal Betic Domain of the western Mediterranean is a typical extensional basin where partial melting appears to have developed in a thinned continental crust after a major phase of lithospheric extension (Platt and Vissers 1989; Vissers et al. 1995; Zeck et al. 1992). Evidence of crustal melting during and after the thinning of the Internal Betics includes migmatites, leucogranitic dykes, calc-alkaline andesites and, most importantly, the high-K calc-alkaline to shoshonitic volcanics of the Neogene Betic basins. The last, represented by the Crd- and Grt-bearing (mineral abbreviations after Kretz 1983) dacites and rhyolites of El Joyazo

(also called Cerro del Hoyazo), Mazarrón, Vera and Mar Menor, are most helpful for understanding in detail the processes of partial melting. In fact, they contain large quantities of crustal material of deep origin, brought to the surface as xenoliths and enclaves in the lavas (e.g., De Larouziere et al. 1988).

The simultaneous occurrence of anatectic volcanics and of abundant portions of their protoliths is absolutely exceptional for crustal domains, and makes these rocks ideal candidates for petrological and chronological studies of the geodynamic evolution of the Betic-Alborán Domain. In fact, although the thinning of the crust had virtually stopped by c. 18–19 Ma (Zeck et al. 1992; Zeck 1996; Platt et al. 1998, 2003; Comas et al. 1999; Platt and Whitehouse 1999), the high-K silicic to intermediate crustal partial melts were erupted much later, between 9 and 6 Ma (Turner et al. 1999 and references therein). This age difference raises two main questions: 1) what are the actual relationships between extension and crustal melting, and 2) could the crustal melts have resided at depth for the whole time between extension and eruption?

In order to answer these questions, and to help refine the geodynamic interpretations of the area, we have dated domains within zircon and monazite in enclaves from the high-K calc-alkaline volcanics by ion microprobe (SHRIMP). In a recent study of the lavas and enclaves from El Joyazo, Zeck and Williams (2002) dated zircons with focus on the information provided by the inherited cores. Conversely, our aim was to define precisely the age of crustal melting and the residence times at depth of anatectic, S-type melts. We have dated samples from both El Joyazo and Mazarrón: the former location has been chosen because it is the most representative and most studied example (Cesare and Gómez-Pugnaire 2001, and references therein), the latter because it is has the largest volume of erupted products and the greatest variety of crustal xenoliths.

The results indicate major differences in the timing of anatexis and magmatism events at the two localities, imposing important constraints on the geodynamic modelling of the Miocene evolution of the Internal Betics. In addition, the comparison of microstructures and ages in monazite and zircon allows a better understanding of the behaviour of these minerals during crustal anatexis at high temperatures.

Geologic setting

The Neogene Volcanic Province (hereafter NVP) is a 200-km-long, NE–SW trending volcanic belt at the southeastern margin of Spain (Ossan 1889; Lopez-Ruíz and Rodríguez-Badiola 1980). It represents the post-collisional volcanism that developed at the northern margin of the Alborán extensional basin. The NVP consists predominantly of calc-alkaline rocks, mostly andesites (Fernández-Soler 1996) and minor high-K calc-alkaline to shoshonitic rocks, ranging in age from

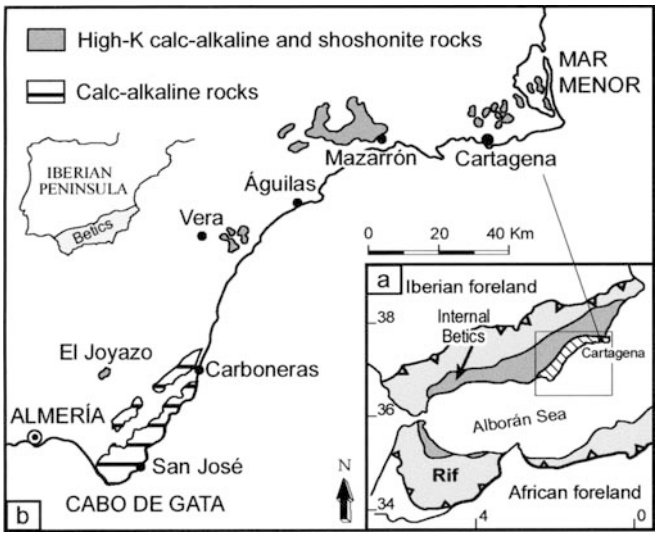

Fig. 1 The Neogene Volcanic Province of SE Spain. **a** Geographic location of the Betic Cordilleras-Rif system and schematic tectonic elements of the Internal Betics (*dark grey*); *box* indicates area enlarged in **b**, *diagonal pattern* indicates the Neogene Volcanic Province. **b** The main edifices of the Miocene volcanics (after López Ruiz and Rodríguez Badiola 1980)

17 to 5 Ma (references in Zeck et al. 1998; Turner et al. 1999). Of particular interest are the high-K calc-alkaline rocks, which occur as scattered, small volcanic edifices (Fig. 1) and are mainly composed of Grt-Crd-bearing dacites.

This work concentrates on two localities where high-K calc-alkaline dacites crop out: El Joyazo and Mazarrón. Material of crustal origin is very abundant in the lavas, up to 15 vol%. The enclaves are medium to coarse-grained granulite-facies rocks, easily recognisable by the typical presence of graphite, euhedral garnet, cordierite porphyroblasts, sillimanite and hercynitic spinel. In addition to these minerals, enclaves at Mazarrón contain abundant andalusite, which is up to 10 cm long and is variably pseudomorphed by sillimanite (Cesare et al. 2002). The enclaves have restitic bulk composition, depleted in silica and enriched in aluminium and iron (e.g. Cesare et al. 1997; Benito et al. 1999). Enclaves range in size from a few tens of centimetres (Fig. 2) down to single xenocrysts, which are the result of restite fragmentation and dispersion in the host lava. The dacite of El Joyazo typically contains cm-sized garnet and cordierite xenocrysts, whereas that of Mazarrón contains also andalusite and sillimanite (Cesare et al. 2002).

There is a general agreement that the dacites and the restitic enclaves are products of crustal anatexis of graphitic metapelites. They represent respectively the leucosome and the melanosome of an erupted migmatite (Zeck 1970), in part contaminated by mafic magmas of mantle origin often observed in the field and as xenoliths in the dacite (Benito et al. 1999). The enclaves testify to a regional scale process of anatexis at depth, not just a localised partial melting event induced by contact with

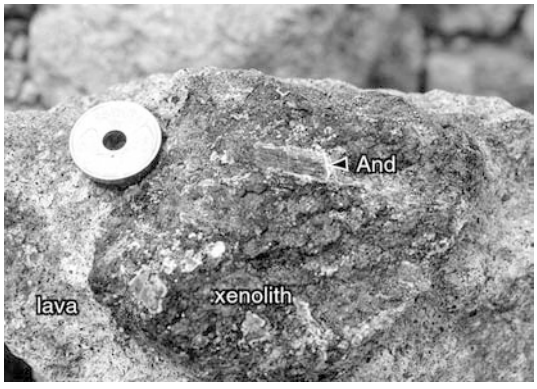

Fig. 2 An example of restitic enclave in the lavas of Mazarrón. The enclave is a partially melted, andalusite-sillimanite-bearing graphitic metapelite, with cm-sized andalusite porphyroblasts (*And*). The coin is approximately 2 cm in diameter

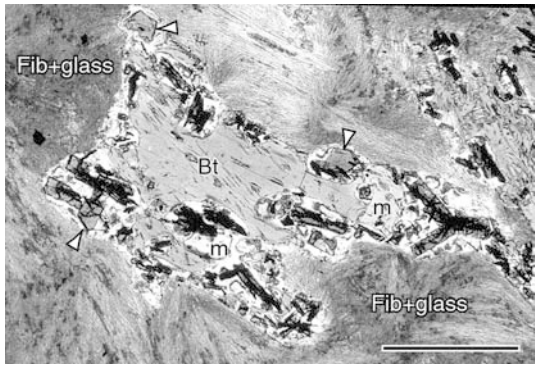

Fig. 3 A crystal of biotite (*Bt*) immersed in a felt of fibrolitic sillimanite (*Fib*) plus glass, in enclave HO02 from El Joyazo. The biotite shows resorbed grain boundaries with partial decomposition into hercynitic spinel (*arrows*), glass (*m*) and ilmenite (*black laths*). Plane-polarised light. *Scale bar* ca. 200 μm

hot magmas. This view, proposed by Zeck (1968), has been supported by detailed microstructural evidence of the syn-anatectic fabric development in the enclaves of El Joyazo (Cesare et al. 1997) and Mazarrón (Cesare and Gómez-Pugnaire 2001).

Direct evidence of partial melting and melt extraction in the enclaves is provided by the occurrence and high abundance of fresh rhyolitic glass (quenched melt, hereafter ''glass'') as primary inclusions (hereafter ''melt inclusions'') in most minerals (Cesare et al. 1997; Zeck 1970). These S-type rhyolitic melts within the enclaves (Cesare 2000; Cesare et al. 2003) are the products of the incongruent melting of the metapelitic protoliths, not the result of melt infiltration from the enclosing dacite. In fact, the enclave-dacite boundary is commonly sharp, without evidence of interaction. In addition, melts in inclusions and intergranular films of enclaves are chemically different from the glass of the dacite host, which have lower Al/Si and higher K/Na (Cesare et al. 1997).

Based on mass balances between melt inclusions, enclaves and potential metapelitic sources, a high degree (35–60 wt%) of melt extraction has been estimated at El Joyazo (Cesare et al. 1997). P–T conditions of partial melting of the enclaves and development of the Grt-Bt-Sil-Pl-melt-graphite ± Crd assemblage have been estimated at 850 ± 50 °C and c. 7 kbar at El Joyazo (Cesare et al. 1997; Cesare and Gómez-Pugnaire 2001). No thermobarometric studies have been performed on the enclaves of Mazarrón before the present work (see below). The only constraint derives from the andalusite-sillimanite transition, which indicates pressures below 4.5 kbar.

Crustal anatexis beneath the NVP has been explained in several ways: emplacement of basaltic magmas (e.g., Zeck 1970), decompression melting (Zeck 1996), and regional heating produced by asthenospheric uprise (e.g., Zeck et al. 1998; Platt and Whitehouse 1999; Platt et al. 2003). As discussed below, recent geophysical data (e.g., Fernandez et al. 1998) seem to favour the last hypothesis, namely that partial melting in the crust and upper mantle beneath the NVP was related to the regional thermal perturbation that accompanied the development of the Alborán Basin.

Petrography

El Joyazo

Crustal enclaves of El Joyazo can be grouped into three types: Grt-Bt-Sil, Crd-Spl and Qtz-Crd enclaves (Zeck 1970). The first type is typically devoid of quartz, is the most abundant, and has been studied in the greatest detail (Cesare and Gómez-Pugnaire 2001, and references therein), as it is considered to be the most representative of the metapelitic crust which partially melted.

Two samples (HO02 and HO33) of Grt-Bt-Sil enclaves, which share many petrographic features, were selected for this study. The mineral composition of sample HO02 is: biotite ($X_{Fe} = 0.58–0.67$, $TiO_2 \sim 5.0$ wt%), plagioclase ($An_{30–40}$), garnet ($Alm_{74–82}Pyp_{10–14}Sps_{1–7}Grs_3$), sillimanite, hercynitic spinel ($X_{Fe} = 0.77–0.80$), K-feldspar, ilmenite, glass and graphite. Sample HO33 includes biotite ($X_{Fe} = 0.62–0.67$, $TiO_2 \sim 5.0$ wt%), plagioclase ($An_{25–33}$), garnet ($Alm_{78–81}Pyp_{10–14}Sps_{1–7}Grs_{2–10}$), cordierite ($X_{Fe} = 0.49$), sillimanite, hercynite ($X_{Fe} = 0.82$), ilmenite, glass and graphite.

Both rocks display a well-developed foliation defined by sillimanite folia, biotite-rich layers and abundant graphite. The foliation is anastomosed around euhedral garnet porphyroblasts and nodular pseudomorphs of fibrolitic sillimanite intermixed with glass, which often appear to replace garnet. Plagioclase-rich domains are elongate parallel to the foliation, alternating with biotite layers. Hercynite is present in very small amounts (< 1%). In sample HO02 it is associated with ilmenite and glass in a reaction rim around biotite (Fig. 3, see also Cesare 2000). Cordierite is present in sample HO33 as cm-sized patchy poikiloblasts, which appear to post-date the development of the main mineral assemblage.

Accessory minerals include apatite, zircon and monazite. Sample HO33 is similar to the enclave studied by Zeck and Williams (2002), although those authors do not mention the presence of glass.

Glass of leucogranitic composition is present in the enclaves as an interstitial phase in layer-parallel films, coatings around garnets, and pockets frequently located at strain shadows (Fig. 4 and Cesare et al. 1997). Glass is also identified as primary melt inclusions in all minerals, including zircon and monazite. This indicates that all minerals crystallized in the presence of a melt phase, i.e., during partial melting (Cesare and Maineri 1999). Microstructures suggest that melt was present: a) during crystallization, by incongruent melting reactions, of the main assemblage (Bt-Grt-Sil); b) during subsequent crystallization of cordierite, and c) after crystallization of restitic phases had ceased, as glass also occurs outside them, as intergranular films.

The mineralogical and chemical features of the dacite hosting the enclaves are described, among others, by Zeck (1968, 1970) and Benito et al. (1999). The lava is porphyritic, with >50 vol.% of rhyolitic glassy matrix, and phenocrysts of plagioclase, biotite, cordierite. It also contains abundant xenocrysts, encompassing the whole mineral assemblage of restites, the most evident being garnet and cordierite.

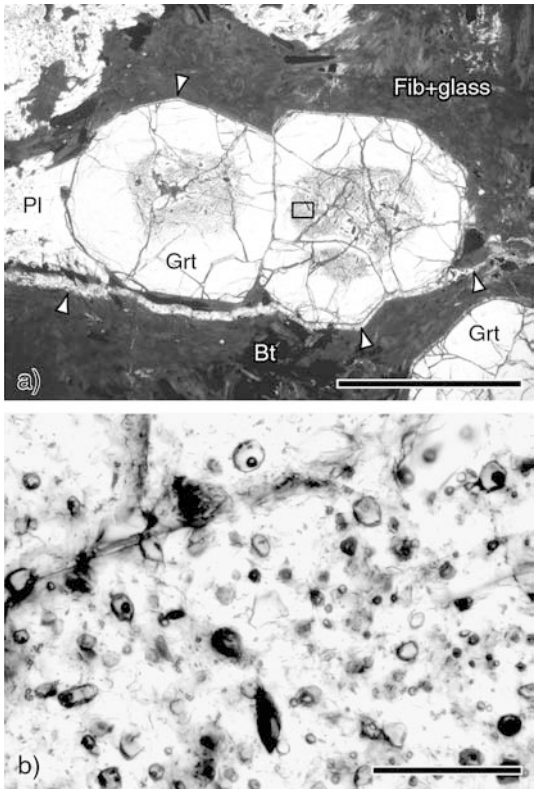

Fig. 4 **a** Sample HO33 from El Joyazo. Two garnet porphyroblasts (*Grt*) coated by a thin film of glass (*arrows*) that passes into a foliation-parallel veinlet on the left-hand side of the image. The cloudy cores of garnets contain primary melt inclusions. Box indicates area enlarged in b. Plane-polarized light. *Scale bar* ca. 3 mm. **b** Close-up of a core of garnet, rich in melt inclusions. Plane-polarised light. *Scale bar* ca. 50 μm

Mazarrón

Compared with those of El Joyazo, enclaves in the lava of Mazarrón display a greater mineralogical variety, but most of them share characteristic features such as the widespread occurrence of cordierite, andalusite and spinel, and smaller amounts of garnet. Contrary to the situation at El Joyazo, garnet commonly has a reaction rim consisting either of Crd + Spl + Kfs, or Bt + Pl/Crd. Melt is also present in the enclaves of Mazarrón, both as interstitial layers and as widespread melt inclusions. The melt inclusions in plagioclase outline a crenulated internal foliation that indicates that partial melting was synchronous with deformation (Cesare and Gómez-Pugnaire 2001).

The investigated sample, MA4-1, is a weakly foliated rock composed of cordierite ($X_{Fe} = 0.49$–0.57), K-feldspar, fibrolitic sillimanite, biotite ($X_{Fe} = 0.71$–0.76, $TiO_2 = 5.3$ wt%), plagioclase ($An_{40–48}$), ilmenite, hercynitic spinel ($X_{Fe} = 0.88$), graphite and peraluminous rhyolitic glass. According to the calibration of Nichols et al. (1992), the Crd-Spl-Sil mineral assemblage constrains the P–T conditions of equilibration in the range 800–900 °C and c. 4 kbar.

The foliation of sample MA4-1 is traced by abundant fibrolite, biotite and graphite, and is overgrown by large poikiloblasts of cordierite up to 1 cm across, often intergrown with K-feldspar. The interstitial glass is often altered and devitrified, whereas the glass occurring within melt inclusions is generally fresh (Fig. 5). Primary melt inclusions are observed in cordierite, feldspars, biotite, ilmenite and apatite. The presence of fine-grained aggregates of euhedral plagioclase, and the local rims of plagioclase at K-feldspar boundaries are suggestive of some in situ crystallization of melt.

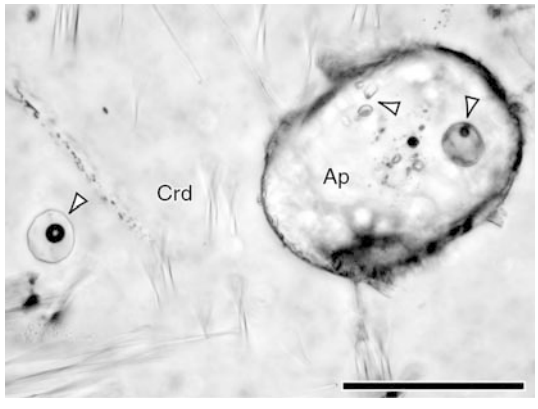

Fig. 5 Photomicrograph of a crystal of cordierite (*Crd*) with an inclusion of apatite (*Ap*) in enclave MA4-1 from Mazarrón. Both minerals contain melt inclusions (*arrows*) with fresh glass (quenched melt) and a shrinkage bubble. Plane-polarized light. *Scale bar* ca. 100 μm

The enclaves are hosted by high-K dacites and shoshonitic latites, containing plagioclase, biotite, orthopyroxene, quartz, ilmenite and magnetite as phenocrysts (Benito et al. 1999).

Analytical techniques

Zircon and monazite for U–Th–Pb analysis were prepared as mineral separates mounted in epoxy and polished down to expose the grain centres. Cathodoluminescence (CL) and back-scattered electron (BSE) images of zircon and monazite were carried out at the Electron Microscope Unit, Australian National University. The CL investigation was performed with a Hitachi S2250-N scanning electron microscope working at 15 kV, a current of ~60 μA and ~20 mm working distance. BSE images of monazite were obtained with a Cambridge S360 scanning electron microscope using a voltage of 20 kV, current of ~3 nA and a working distance of ~20 mm.

U–Th–Pb analyses were performed using a sensitive, high-resolution ion microprobe (SHRIMP II) at the Research School of Earth Sciences (RSES). Instrumental conditions and data acquisition were generally as described by Compston et al. (1992). The data were collected in sets of seven or six scans throughout the masses. The measured $^{206}Pb/^{238}U$ ratio was corrected using reference zircons from a gabbro of the Duluth Complex in Minnesota (AS3, 1099 Ma) and reference monazite from Thompson mine, Manitoba (1766 Ma). A zircon of known composition (SL 13) has been used to determine the U content of zircon. The isobaric interference on mass 204, which is often encountered in SHRIMP analysis of monazite, was not observed in these samples. Zircon and monazite data were corrected for common Pb on the basis of the measured $^{207}Pb/^{206}Pb$ ratios or ^{204}Pb (El Joyazo monazite) as described in Compston et al. (1992). Owing to the young age and the low U content of the samples, some analyses have a high proportion of common Pb. However, in absolute amount, the common Pb content of the samples is similar to that of the common Pb-free standard. This indicates that the common Pb is mainly surface Pb, the composition of which is assumed to be that of Broken Hill Pb ($^{204}Pb/^{206}Pb = 0.0625$; $^{207}Pb/^{206}Pb = 0.9618$; $^{208}Pb/^{206}Pb = 2.229$). If an average Miocene crustal Pb composition is assumed, the ages do not change significantly. Ages were calculated using the software Isoplot/Ex (Ludwig 2000). Uncertainties in mean ages are listed at the 95% confidence level, whereas single analyses in both text and tables are reported with 1σ error.

Microstructural and U–Th–Pb analysis of zircon and monazite

El Joyazo

Zircon

Zircon grains in the two enclaves from El Joyazo are small (≤100 μm), euhedral to subhedral, colourless to pale pink and mainly clear (Fig. 6). The zircon crystals are often inclusion-rich, with two major types of inclusions: a) black micro-inclusions of graphite, b) rounded melt inclusions. Because of their small size, electron microprobe analysis of the melt inclusions could not produce analyses free of zircon contamination. However, given the proportions of SiO_2, Al_2O_3, Na_2O and K_2O, these mixed analyses clearly indicate a linear combination between zircon and a phase with the composition of a granitic melt.

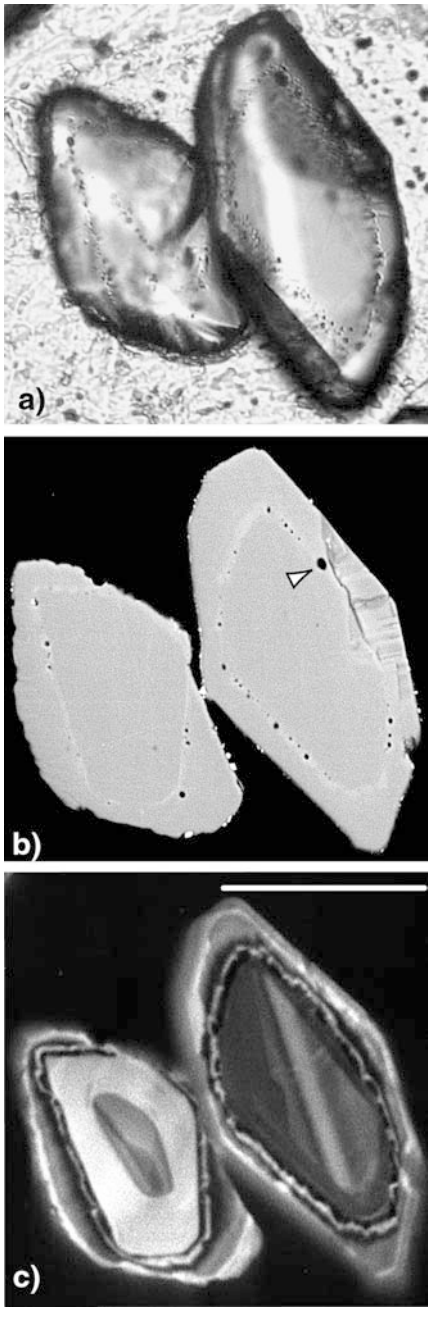

Fig. 6 Zircons from El Joyazo enclave. **a** Transmitted light photomicrograph of crystals with an evident core and overgrowth. Microinclusions are concentrated at the core-overgrowth interface. **b** Backscattered SEM image of the same crystals. The core-rim interface is outlined by a slightly lighter band, and microinclusions (*black spots*) are located inside and immediately outside this band. Qualitative EDS microanalysis on the largest inclusion (*arrow*) confirms that it contains a rhyolitic glass. **c** Cathodoluminescence image of the same crystals. Note the different zoning pattern of cores and overgrowths and the light irregular band at their interface. Scale bar: 65 μm

Cathodoluminescence images (Figs. 6c, 7) reveal complex zoning characterized by two major concentric zones, i.e. core and overgrowth, which are often visible

even under optical microscopy. The cores have oscillatory and/or sector zoning with variable width and contrast in emission between the different bands. This kind of variability is typical of a detrital population with various sources, mainly of magmatic origin, as indicated by the oscillatory zoning of most of the zircon cores. The zoning pattern of the cores is truncated by the overgrowths. The surface of the cores appears irregular and pitted, as expected in grains that underwent either mechanical abrasion due to transport or chemical corrosion by fluid or melt (e.g., Vavra et al. 1996; Williams 2001). The width of the overgrowths ranges up to 30 μm and is generally greater at the zircon tips. Overgrowths present a simple zoning pattern with an internal darker band followed by an external lighter band. The boundary between core and overgrowths is marked by a micrometer-wide bright band that follows the irregular surface of the cores. The significance of this band is difficult to establish because its reduced thickness prevents any isotopic or chemical analysis. Vavra et al. (1996) observed a similar band around zircon cores and suggested that it might be due to recrystallization. In our case, comparison of BSE and CL images in Fig. 6 reveals that microinclusions of melt are located internally with respect to this bright band, indicating that they were trapped at the initial stage of zircon overgrowth and that the bright band cannot be the product of recrystallization.

In attempt to date the granulite facies metamorphism and partial melting, the SHRIMP analyses were concentrated on the zircon rims (Fig. 7). These rims have medium U content (160–640 ppm), but low Th content (0.5–5 ppm), leading to an extremely low Th/U of 0.005–0.015 (Table 1). These values are often observed in zircon formed during anatexis (e.g., Vavra et al. 1996; Williams et al 1996; Rubatto et al. 2001) and are probably due to the simultaneous growth of monazite (see below), a Th-rich mineral. The $^{206}Pb/^{238}U$ ages of 15 rims are in the range 8.8–10.4 Ma. No age difference was detected between the two samples or between the outer or inner part of the overgrowths, in the few cases in which they were wide enough to allow a SHRIMP analysis. In a total $^{238}U/^{206}Pb$ vs. $^{207}Pb/^{206}Pb$ plot (Fig. 8a) the overgrowth analyses fall on a mixing line with common Pb, which intersects the concordia curve at 9.63 ± 0.26 Ma. One rim analysis plots off the mixing line and yields an age of 8.28 ± 0.28 Ma (1σ). This analysis is excluded from the calculation of the mean age.

The few cores analysed have much higher Th contents and higher Th/U (0.7–1.8), similar to values often reported for magmatic zircon (e.g., Vavra et al. 1996; Williams et al 1996; Rubatto et al. 2001; Zeck and Williams 2002). They have concordant ages at c. 620 Ma, 2085 Ma and 2670 Ma. These cores are interpreted as inherited detrital zircon crystals from the sedimentary precursor of the enclave. The ages of the cores are consistent with the more comprehensive data set of Zeck and Williams (2002) on inherited zircon cores from the El Joyazo enclaves and dacitic lava.

Monazite

The monazite crystals recovered from the El Joyazo enclaves are relatively small (50–150 μm), dark yellow, anhedral and mainly turbid because they are rich in inclusions of glass, biotite, graphite and apatite (Fig. 9). They occasionally form aggregates with cordierite. The zoning pattern observed in BSE imaging consists of a bright core (trace element rich) with patchy zoning and a dark rim (trace element poor) that is often lacking any significant zoning (Fig. 9b). The core-rim boundary is transitional. Inclusions are disseminated throughout the crystals and, in contrast to those in zircon, they do not follow the zoning. Among the inclusions large enough to be identified with an optical microscope, the most common are apatite, biotite, glass and graphite.

The monazite crystals have Th content variable according to the BSE zoning: the bright cores are richer in Th (14–17 ThO_2 wt%) with respect to the darker rims (1–5 ThO_2 wt%). No age difference has been detected between cores and rims (Table 2). All the analyses, with the exception of one, cluster on concordia defining an average age of 9.74 ± 0.21 Ma (Fig. 8b), in agreement with the zircon data.

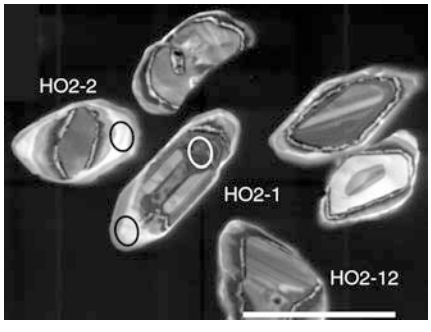

Fig. 7 Cathodoluminescence image of zircons from the El Joyazo enclave, with *circles* indicating the SHRIMP pits. The grains on the right-hand side are the same as in Fig. 6. *Scale bar* 100 μm. Labels as in Table 1

Mazarrón

Zircon

Most of the zircon crystals recovered from the Mazarrón enclave are subhedral with rounded tips. They generally preserve some crystal faces. A small portion of the grains (c. 20%) preserves euhedral, elongated shape with sharp facets and pointed tips. The zircon crystals are mainly colourless or pale pink and transparent. The CL investigation (Fig. 10) reveals a pattern similar to that of El Joyazo enclaves, with oscillatory-zoned magmatic cores and irregular overgrowths with no or weak zoning. In this sample the overgrowths are even smaller, only occasionally reaching a dimension that can be analysed

Table 1 Zircon SHRIMP U–Th–Pb data

	U (ppm)	Th (ppm)	Th/U	com Pb (%)	Total $^{238}U/^{206}Pb \pm 1\sigma$		Total $^{207}Pb/^{206}Pb \pm 1\sigma$		Age $^{206}Pb/^{238}U \pm 1\sigma$	
El Joyazo xenoliths[a]										
HO2-1.1 o	231	1.8	0.008	7.2	722.1	24.2	0.1122	0.0061	8.28	0.28
HO2-1.2 c	1176	865.7	0.736	0.5	13.2	0.2	0.0612	0.0003	469	6
HO2-2.1 o	296	1.2	0.004	8.8	621.0	18.2	0.1268	0.0066	9.46	0.29
HO2-4.1 o	299	0.9	0.003	9.8	629.9	16.6	0.1361	0.0097	9.22	0.27
HO2-5.1 o	549	2.4	0.004	1.7	608.8	13.2	0.0615	0.0038	10.40	0.23
HO2-5.2 c	277	403.4	1.458	3.5	1.9	0.0	0.1819	0.0006	2618	30
HO2-6.1 o	187	0.5	0.003	6.1	659.4	20.7	0.1020	0.0062	9.18	0.30
HO2-7.1 o	398	1.6	0.004	4.3	611.1	11.7	0.0858	0.0044	10.08	0.20
HO2-8.1 o	220	1.2	0.006	17.6	600.7	16.5	0.2077	0.0125	8.83	0.28
HO2-8.2 c	60	105.7	1.771	1.3	2.6	0.1	0.1301	0.0010	2059	43
HO2-9.1 o	481	2.8	0.006	1.8	655.3	12.0	0.0628	0.0034	9.65	0.18
HO2-10.1 o	328	1.5	0.004	9.9	630.3	14.7	0.1368	0.0081	9.21	0.23
HO33-1.1 o	309	1.2	0.004	3.2	631.1	33.7	0.0752	0.0051	9.88	0.53
HO33-2.1 o	307	1.5	0.005	5.8	636.4	14.6	0.0995	0.0054	9.53	0.23
HO33-3.1 o	270	1.3	0.005	11.5	579.8	14.5	0.1513	0.0080	9.83	0.26
HO33-4.1 o	403	2.9	0.007	29.8	467.1	11.3	0.3193	0.0148	9.68	0.32
HO33-5.1 o	322	1.1	0.004	3.9	677.8	18.6	0.0820	0.0056	9.13	0.26
HO33-6.1 o	331	4.8	0.015	17.4	513.3	12.5	0.2058	0.0099	10.36	0.29
HO2-11.2 o	639	3.7	0.006	4.3	673.1	12.4	0.0800	0.0053	9.22	0.18
Mazarron xenolith										
MA4.1-1.1 mix	1097	193.2	0.176	3.1	255.7	5.1	0.0776	0.0027	24.4	0.5
MA4.1-2.1 mix	279	23.0	0.083	2.6	55.7	1.3	0.0735	0.0031	112	3
MA4.1-3.1 mix	1524	100.6	0.066	0.6	24.5	0.3	0.0552	0.0006	256	3
MA4.1-5.1 mix	534	15.2	0.028	80.8	31.9	0.7	0.7868	0.0190	38.6	4.3
MA4.1-6.1 mix	639	10.4	0.016	76.1	79.3	1.8	0.7437	0.0132	19.4	1.3
MA4.1-7.1 mix	301	5.8	0.019	73.9	39.8	0.7	0.7237	0.0105	42.1	2.0
MA4.1-8.1 o	531	13.0	0.024	11.3	684.8	26.6	0.1524	0.0089	8.34	0.34
MA4.1-9.1 o	1221	41.3	0.034	14.7	593.2	12.4	0.1832	0.0065	9.27	0.21
Mazarron volcanic										
MA91-1.1	1655	631	0.381	4.0	698.6	12.7	0.0856	0.0034	8.85	0.16
MA91-2.1	2740	954	0.348	4.4	652.6	9.8	0.0893	0.0024	9.44	0.14
MA91-3.1	5362	332	0.062	0.9	697.1	13.8	0.0580	0.0013	9.15	0.18
MA91-4.1	1827	929	0.508	1.8	722.8	11.9	0.0659	0.0019	8.75	0.15

[a] *c* Core; *o* overgrowth; *mix* physical mixture of two domains

by SHRIMP (25 μm). Only in a few crystals do the overgrowths display two bands with different CL emission as observed at El Joyazo. A bright, thin band marking the core-overgrowth boundary is not as visible here because most of the overgrowths have strong CL emission. However, the very irregular surface of the boundary to the core is also present in this sample. As for El Joyazo, the irregular surface and occasionally truncated zoning pattern of the cores suggest that the crystals were corroded or abraded before formation of the overgrowth.

Zircon was also recovered from one Mazarrón dacite sample. These crystals have a different appearance from those from the enclave: they are euhedral and elongated (aspect ratio up to 4:1), clear and pink. The zoning patterns are characterized by cores with magmatic zoning truncated by overgrowths that also show oscillatory zoning (Fig. 10). The width of the overgrowths is proportional to the aspect ratio, with wider overgrowths on the more elongated grains. The core-overgrowth boundary is often irregular and marked by a CL-bright band. These zoning features suggest that the cores were chemically corroded or physically abraded, whereas the overgrowth crystallized in a magmatic environment (oscillatory zoning) where an elongated shape was preferred. An elongated crystal shape is quite typical of zircons from volcanic rocks.

Because of the small dimension of the zircon overgrowths in the Mazarrón enclave, most of the attempted analyses resulted in a physical mixing with the cores. Microscopic investigation after isotopic analysis confirmed that most SHRIMP pits sampled core and rim together. Only in two cases were the SHRIMP pits located completely on the overgrowths. These analyses (#8.1 and #9.1 in Table 1) yielded ages of 8.34 ± 0.34 and 9.27 ± 0.21 Ma (1σ). The Th-U composition of these overgrowths is different from the El Joyazo samples, particularly because of slightly higher Th content and thus higher Th/U (0.02–0.03) than at El Joyazo. The other analyses, which are mixed with cores, yielded older ages scattering between 20 and 600 Ma. All the analyses are discordant, in line with physical mixing of two domains: old, inherited cores and young overgrowths. In the mixed analyses, Th and Th/U are higher than in the overgrowths, indicating that the cores have a magmatic Th-U composition (Th >10 ppm and Th/U >0.5, see

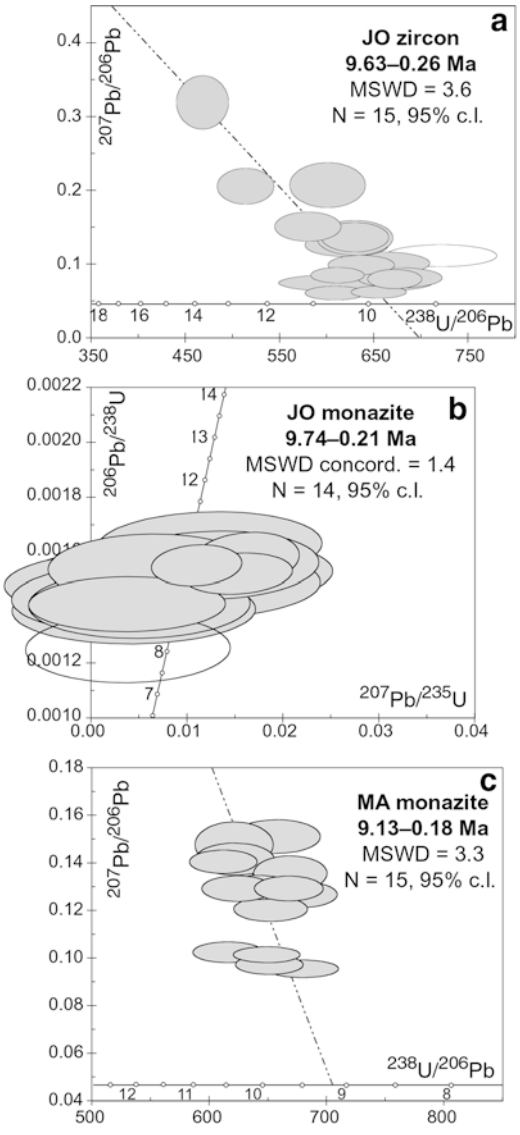

Fig. 8a–c Concordia diagrams representing the U-Pb data from El Joyazo and Mazarrón enclaves. Error ellipses represent 1σ errors. Ages are at 95% confidence level. Data plotted as empty ellipses are excluded from the age calculation. See text for discussion

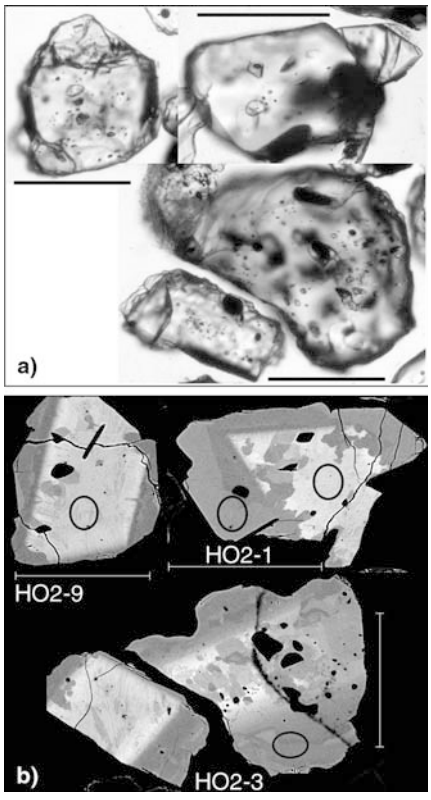

Fig. 9 Monazite from El Joyazo enclaves. **a** Transmitted light photomicrograph of crystals rich in inclusions, which consist of glass, biotite, graphite and apatite. Note that no core-overgrowth structure is visible and that inclusions occur throughout the grains, but are more abundant at grain cores. **b** BSE images of the same crystals as in **a**, with bright patchy cores and dark rims. The boundary between these two domains is transitional. The *circles* indicate the SHRIMP pits. Labels as in Table 1. Scale bars: 100 μm

also Vavra et al. 1996, Williams et al 1996, Rubatto et al. 2001, Zeck and Williams 2002).

Only four analyses were carried out on the zircon from the host lava (Table 1), and all of them are located on oscillatory-zoned overgrowths. The overgrowths have Th/U ratios >0.05, as expected in magmatic zircon. The ages obtained scatter around 9 Ma (9.06 ± 0.53 Ma) and are consistent with the two analyses from zircon overgrowths in the Mazarrón enclave. These ages are in agreement with the Ar/Ar data obtained on biotite by Turner et al. (1999).

Monazite

Because of the limited number of analyses that could be obtained on zircon overgrowths, the Mazarrón enclave was screened for monazite. The small sample (<1 kg) yielded 40–50 monazite crystals or crystal fragments, which are small (<100 μm), partly euhedral, clear and vary from colourless to pale yellow. The BSE investigation (Fig. 11) revealed two types of monazite domains: a) cores with low BSE emission, rich in inclusions such as in the sample from El Joyazo, and lacking any polygonal zoning; b) bright rims with traces of sector or oscillatory zoning.

The cores differ from the rims mainly because of higher Th content (Table 2) and thus Th/U. Similarly to the monazite from El Joyazo, no difference was detected in terms of U/Pb between cores and rims. In the total $^{238}U/^{206}Pb$ vs. $^{207}Pb/^{206}Pb$ diagram, the 15 analyses plot along a mixing line with common Pb, which defines a $^{206}Pb/^{238}U$ age of 9.13 ± 0.18 Ma (Fig. 8c).

Age interpretation

The isotopic analyses were mainly carried out on overgrowths or external rims with the intention of dating the late history of these rocks. Therefore, our discussion focuses on the young ages obtained, without commenting

Table 2 Monazite SHRIMP U–Th–Pb data

	U (ppm)	ThO_2 wt%	Th/U	% com Pb	$^{206}Pb/^{238}U \pm 1\sigma$		$^{207}Pb/^{235}U \pm 1\sigma$		Age $^{206}Pb/^{238}U \pm 1\sigma$	
El Joyazo xenoliths[a]										
HO2-1.1 r	2223	2.5	9.8	7	0.0014	0.0001	0.004	0.005	9.02	0.35
HO2-1.2 c	7909	14.2	15.8	13	0.0015	0.0001	0.005	0.006	9.58	0.35
HO2-2.1 r	4623	1.3	2.5	5	0.0016	0.0001	0.013	0.005	10.02	0.31
HO2-3.1 r	6143	2.1	3.0	10	0.0014	0.0001	0.004	0.005	9.30	0.32
HO2-2.2 r	6272	2.9	4.1	6	0.0016	0.0001	0.006	0.004	10.01	0.32
HO2-4.1 c	7400	17.4	20.7	11	0.0015	0.0001	0.012	0.005	9.86	0.34
HO2-5.1 c	6596	14.1	18.8	10	0.0016	0.0001	0.012	0.005	10.51	0.32
HO2-5.2 r	2910	3.0	9.1	8	0.0013	0.0001	0.004	0.004	8.10	0.32
HO2-6.1 r	6435	1.2	1.7	2	0.0016	0.0000	0.011	0.002	10.03	0.21
HO2-7.1 r	4101	2.2	4.7	9	0.0015	0.0001	0.005	0.006	9.56	0.38
HO2-8.1 r	3885	3.0	6.8	7	0.0015	0.0001	0.011	0.005	9.58	0.33
HO2-9.1 c	7280	13.5	16.3	12	0.0014	0.0001	0.005	0.005	9.15	0.30
HO33-1.1 c	5931	4.5	6.7	3	0.0016	0.0000	0.016	0.002	10.16	0.24
HO33-2.1 c	5940	3.4	5.0	9	0.0014	0.0000	0.004	0.004	9.16	0.28
HO33-3.1 c	7613	4.8	5.6	2	0.0015	0.0000	0.015	0.002	9.83	0.21

	U (ppm)	ThO_2 wt%	Th/U	% com Pb	Total $^{238}U/^{206}Pb \pm 1\sigma$		Total $^{207}Pb/^{206}Pb \pm 1\sigma$		$^{206}Pb/^{238}U \pm 1\sigma$		Age $^{206}Pb/^{238}U \pm 1\sigma$	
Mazarrón xenoliths												
MA4.1-1.1 c	1983	3.4	15	11	657.3	15.2	0.151	0.003	0.00135	0.00003	8.67	0.20
MA4.1-2.1 r	3809	15.1	35	10	621.8	13.6	0.142	0.003	0.00144	0.00003	9.28	0.21
MA4.1-3.1 r	3452	11.6	30	9	624.2	12.5	0.130	0.002	0.00146	0.00003	9.38	0.19
MA4.1-4.1 c	3970	3.2	7	6	615.9	12.2	0.103	0.002	0.00152	0.00003	9.81	0.20
MA4.1-5.1 r	4582	9.0	17	8	652.6	12.9	0.121	0.002	0.00141	0.00003	9.06	0.18
MA4.1-6.1 r	2220	6.8	27	11	621.3	13.7	0.148	0.004	0.00143	0.00003	9.22	0.21
MA4.1-7.1 r	6436	11.2	15	6	651.1	11.8	0.098	0.002	0.00145	0.00003	9.34	0.17
MA4.1-7.2 c	4218	3.7	8	10	612.1	11.8	0.141	0.002	0.00146	0.00003	9.44	0.18
MA4.1-8.1 c	4793	4.2	8	9	668.0	12.0	0.130	0.002	0.00136	0.00002	8.76	0.16
MA4.1-8.2 r	9375	12.4	12	5	679.5	12.5	0.096	0.002	0.00139	0.00003	8.96	0.17
MA4.1-9.1 r	3680	9.7	23	9	642.0	12.8	0.130	0.002	0.00142	0.00003	9.12	0.18
MA4.1-10.1 r	2581	5.7	19	9	646.2	13.6	0.130	0.002	0.00141	0.00003	9.06	0.19
MA4.1-11.1 r	4031	11.1	24	9	676.7	13.2	0.127	0.002	0.00135	0.00003	8.68	0.17
MA4.1-12.1 c	5168	4.0	7	6	649.0	11.6	0.102	0.001	0.00145	0.00003	9.32	0.17
MA4.1-13.1 r	4233	12.4	26	10	669.0	12.8	0.136	0.003	0.00135	0.00003	8.68	0.17

[a] *c* Core; *r* rim

on the source material of the enclaves, a topic which has been dealt with in more detail by Zeck and Williams (2002).

In the El Joyazo samples, the age of the zircon overgrowths and that of the monazite are identical within error (9.63 ± 0.26 and 9.74 ± 0.21 Ma, respectively). The presence of numerous melt inclusions at the core-overgrowth interface in the zircon indicates that the overgrowths formed in the presence of a melt phase, i.e., during partial melting. Moreover, the Th content below 10 ppm, the Th/U < 0.015 and the absence of oscillatory zoning are in line with formation of the overgrowths during high-temperature (HT) metamorphism in the presence of monazite (e.g. Vavra et al. 1996; Williams et al. 1996; Rubatto et al. 2001; Williams 2001). It is thus concluded that the zircon overgrowths formed during a partial melting event under granulite-facies conditions.

Monazite also grew during partial melting, as testified by the melt inclusions that it commonly contains. Given the HT at which the enclaves equilibrated (850 ± 50 °C) and the pelitic composition of their protoliths, it is not surprising that the partial melting recorded by the zircon also induced growth of monazite. The zoning observed in the monazite is likely to reflect a change in trace

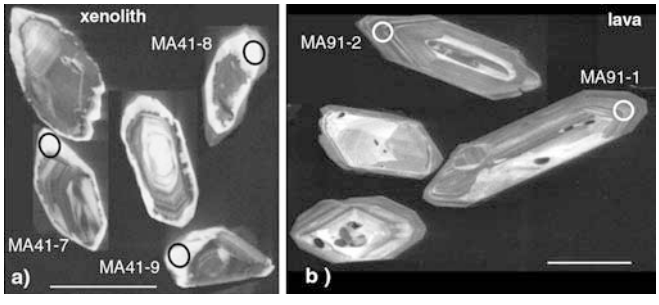

Fig. 10 Cathodoluminescence images of zircons from Mazarrón. The *circles* indicate the SHRIMP pits. **a** Enclave. The bright rims are often too small for a SHRIMP analysis, resulting in mixed ages. **b** Lava. Note the presence of cores and the oscillatory zoning of the overgrowths. *Scale bars* 100 μm. Labels as in Table 2

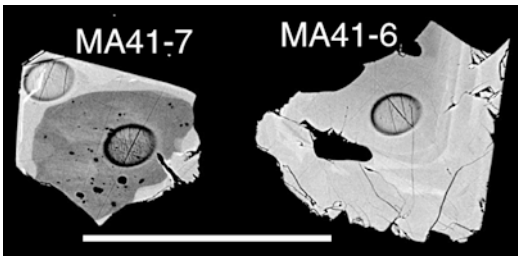

Fig. 11 BSE image of monazites from the Mazarrón enclave. All analyses yielded the same age, regardless of the core-rim structure. The *circles* indicate the SHRIMP pits. Labels as in Table 2. Scale bar represents 100 μm

element composition of the anatectic melt during monazite growth.

The age of anatexis recorded by zircon and monazite from El Joyazo samples is significantly older than the age of 8.34 ± 0.45 Ma determined on zircon overgrowths from a similar enclave from the same locality by Zeck and Williams (2002). This may seem inconsistent, because the rocks investigated in the two studies are almost identical. We propose two possible explanations for such an apparent discrepancy. The first is that age data of Zeck and Williams (2002) may be affected by mixing. In fact, their results scatter in age between 9.3 ± 0.6 and 7.0 ± 0.6 Ma (1σ) and the probability plot of the data suggests that they may represent a bimodal population. Zeck and Williams (2002) calculated an average age with a relatively low MSWD of 2, probably because of the large uncertainty on each analysis. It cannot be excluded that the age of 8.34 ± 0.45 Ma that they calculated is an artefact due to mixing of a ~9.5 Ma population and a younger component of age < ~7 Ma, maybe as young as the dacite lava (6.33 ± 0.15 Ma; Zeck and Williams 2002). An age of 9.5 ± 0.5 Ma (1σ) was also obtained from one euhedral, oscillatory zoned zircon from the dacitic lava (Zeck and Williams 2002), further supporting the hypothesis of a major melting event of this age.

An alternative possibility is that the different ages are both correct, and that they represent different times at which zircon growth (as a response to melting) occurred. The Bt-Grt-Sil enclaves of El Joyazo represent fragments of a coherent crystalline basement constituting the lower crust in the area (Cesare et al. 1997; Cesare and Gomez-Pugnaire 2001). Therefore, we suggest that the thermal perturbation, which produced anatexis on a regional scale, may have been recorded in (slightly) different times in different places. The very similar enclaves would therefore represent samples of different portions of this crystalline basement, either located enough apart, or having slightly different bulk compositions, to record the partial melting event at different times.

The slightly younger ages obtained in this study on one of the zircon overgrowths (8.28 ± 0.28 Ma, 1σ) and one monazite (8.10 ± 0.32 Ma, 1σ) from El Joyazo could be explained by small amounts of recent Pb loss from originally 9.6 Ma old grains. Recent Pb loss might have occurred along fractures or grain boundaries even at low temperatures, if induced by fluids (e.g., Teufel and Heinrich 1997). However, such younger age detected in both zircon and monazite is remarkably similar to the age proposed by Zeck and Williams (2002) for HT metamorphism in another enclave from El Joyazo (8.34 ± 0.45 Ma). Under the hypothesis given above that this age is correct, the two young ages found in our samples could be recording a further anatectic event in the source of the enclave. This possible second melting event produced only limited zircon growth or recrystallization and did not cause a widespread resetting of the U-Pb system in our samples. Even monazite, which is generally more sensitive to metamorphism, recorded this second event only occasionally (one analysis in our study). It is worth noting that the ages at c. 8 Ma have been obtained in sample HO02, which contains evidence of biotite melting to hercynitic spinel (Fig. 3). According to Cesare (2000), this microstructure testifies to a further melting event that post-dated the development of the main assemblage Bt-Grt-Sil-Pl-melt and took place at c. 900–950 °C and ≥5 kbar. Thus, we suggest that the zircon and monazite overgrowths at c. 8 Ma may record the incongruent melting of biotite that is observed in some enclaves.

The amount of zircon overgrowth in the Mazarrón enclave is smaller than that observed at El Joyazo. However, the analysed overgrowths have the same zoning and Th-U features as at El Joyazo. Even if the inclusion relationships are not as clear as at El Joyazo, formation of overgrowths is again attributed to anatexis related to granulite-facies metamorphism. The age of this event (9.13 ± 0.18 Ma) is much better defined in the monazite which, like that at El Joyazo, was more reactive during the HT metamorphism.

The zircon overgrowths from the lava of Mazarrón have shape, zoning and, in most cases, Th-U composition that distinguishes them from the metamorphic overgrowths in the enclaves. Their features are similar to what observed in magmatic zircon from different lithologies, particularly volcanics (e.g., Zeck and Williams 2002). Their age is thus interpreted as dating the crystallization of the dacite at 9.06 ± 0.53 Ma.

Discussion

Residence times of anatectic magmas

At El Joyazo, crystallization of the dacite enclosing the enclaves that we investigated has been dated by Turner et al. (1999) at 6.2 ± 0.4 Ma by Ar/Ar dating of biotite, and by Zeck and Williams (2002) at 6.33 ± 0.15 Ma by SHRIMP U-Pb analysis of zircon. The comparison of ages from restitic enclaves and host dacite indicates that crustal anatexis recorded by growth of zircon and monazite occurred c. 3 m.y. prior to eruption at El Joyazo. We interpret these data as an indication that after crustal melting the partially melted rocks

(migmatites) remained at temperatures of 850 ± 50 °C for c. 3 m.y., i.e., that anatectic magmas resided at depth for the same period.

This interpretation might be questionable for two interrelated reasons. First, because we infer values of residence times which would seem at odds with those ten times shorter (e.g., 300 ka at Long Valley, California) that are reported among the most protracted residence periods (e.g., Reid et al. 1997; Davies and Halliday 1998; Heath et al. 1998). Second, because we propose a continuous presence of melt on the basis of an episodic geochronologic record (9.7, 8.2 and 6.3 m.y.) provided by zircon and monazite.

We believe that our interpretations are in agreement both with the available field and petrologic data, and with theoretical reasoning. In fact, a prolonged presence of melt in the enclaves is testified by the occurrence of melt inclusions in all the minerals of the main assemblage (Bt, Grt, Pl, including zircon and monazite), by melt inclusions in cordierite postdating the main paragenesis, and by intergranular melt recording the end of crystallization. Throughout the enclaves, the melt is fresh and shows no evidence of crystallization: this suggests that enclaves remained above solidus temperatures from early melt entrapment until eruption. Additional support to continuous melt presence at depth is given by the calc-alkaline volcanics of the NVP, which record a prolonged magmatic activity (17 to 5 m.y., e.g., Zeck et al. 1998, and references therein) and a systematic chemical variation (Benito et al. 1999).

There is no obstacle to achieving these long residence times in an appropriate geodynamic setting which allows long lasting, high thermal regimes to be maintained. Numerical models of the thermal evolution of orogens characterised by delamination of the lithospheric mantle (Arnold et al. 2001) support the idea that areas of extensive crustal melting can be maintained for timescales of > 100 m.y. when hot asthenosphere is placed at the base of the crust. In these conditions, melting of the crust should commence shortly (1–10 Ma) after asthenospheric rise. The age of crustal melts in the NVP is c. 10 Ma younger than the lithospheric thinning in the area, in agreement with the timescales predicted by Arnold et al. (2001).

Alternatively, or along with the previous process, long-lived thermal anomalies can also be produced by repeated intrusion of mantle-derived basalt into the deep crust. As modelled by Annen and Sparks (2002), these anomalies can account for protracted conditions of partial melting and magma residence in the fertile pelitic crust, and can take several million years to decay after intrusion is finished. These zones are predisposed to remelt if a subsequent magmatic episode initiates. The results of Annen and Sparks (2002), obtained for moderate geothermal gradients and in the presence of cool lithospheric mantle, suggest that in regions of higher geothermal gradients and shallow asthenosphere, such as the Internal Betics, thermal anomalies may be even more pronounced and their timescale longer. A case study describing a period of melt production and crystallization lasting > 25 Ma is documented in the Proterozoic province of central Australia (Reynolds Range, Williams et al. 1996; Rubatto et al. 2001). Rubatto et al. (2001) suggested that such a prolonged melting occurred during prograde and retrograde metamorphism. Their suggestion requires a long lasting HT regime during which the relatively high geotherm present in the area at the time of metamorphism reached a nearly steady state, as supported by thermal modelling. Another example of melting extended over a period of time of c. 6 m.y. is given by Keay et al. (2001) in their study of the Neogene evolution of Naxos.

Because the Alborán sea is an extensional basin active from the Early Miocene up to present day (e.g., Comas et al. 1999), and characterised by the presence of shallow asthenospheric mantle below a thinned crust, we propose a similar situation of long lasting partial melting in the lower crust beneath the NVP. As discussed below, the high thermal regime in this region can be traced back to c. 17 Ma and is, as indicated by present-day geophysical data (Fernández et al. 1998; Zappone et al. 2000), still active.

As concerns the episodic geochronological record provided by zircon and monazite, this can be fully consistent with a framework of continuous melt presence, if the episodic character of melting reactions involving these minerals is taken into account. In fact, in a continuous P–T loop, rocks commonly experience major mineralogical changes by episodic, discontinuous reactions, and if P–T conditions persist at fairly constant values, even for a long period, rocks very likely record little or no reaction. However, the mechanism of repetitive intrusions of basalt in the lower crust (Annen and Sparks 2002) raises an alternative possibility, i.e., that melt was not present in the enclaves of El Joyazo for the whole time interval between 9.7 Ma and eruption at 6.3 Ma. As a consequence, the enclaves could have undergone a first episode of melting, then were subsequently cooled below their solidus temperature, and were remelted just, or more times, before dacite eruption. We cannot rule out the possibility of repeated melting episodes. However, the above reported microstructural evidence in favour of a continuous presence of melt, the lack of back-reaction microstructures (Kriegsman and Hensen 1998) indicating repeated heating and cooling events, as well as the geochronological record obtained from zircon and monazite in this study, are more easily explained in terms of prolonged melt presence.

Our data help to constrain the hypothesis of Zeck and Williams (2002), who suggested a 2–3 m.y. residence time on the basis of a limited number of zircon analyses. Our inferred residence times of 3 m.y. may be a minimum estimate, because we cannot exclude the possibility that a larger number of enclave samples would provide zircon and monazite ages (much) older than 9.7 Ma. In adjacent areas, Zeck et al. (1998) have found evidence for a protracted magmatic development of c. 5 m.y. for

calc-alkaline andesites prior to their eruption at c. 11 Ma.

This research also adds information on the timescales of equilibration processes at high temperature. Although the restitic enclaves have remained in the presence of melt for c. 3 m.y. at temperatures of 850 ± 50 °C, they show clear examples of disequilibrium. They include the age inheritance preserved in zircon, the preservation of compositional zoning in the largest (radius > 2 mm) crystals of garnet, the variable degree of crystallinity of graphite (Cesare and Maineri 1999), and the lack of coarsening of fibrolite to sillimanite (Cesare et al. 2002). These examples demonstrate that timescales of c. 3 m.y. of temperatures in excess of 800 °C in the presence of melt are sufficient neither to achieve intracrystalline homogenization to distances from > 10 μm (zircon) to > 2 mm (garnet), nor to recrystallize graphite to a fully ordered structure. In the case of garnet, this behaviour is in agreement with available data on Mn diffusion (Chakraborty and Ganguly 1991), which indicate that complete homogenization of growth profiles of garnets with radii of 2 to 3 mm should take 4 to 8 Ma at 800 °C, and 1 to 2.5 Ma at 850 °C.

The long residence time proposed for the El Joyazo enclaves implies a high closure temperature, slow Pb diffusion and a refractory behaviour of zircon and monazite under prolonged HT conditions (850 ± 50 °C). This is expected for zircon, in which Pb diffusion at this timescale is not expected below 900–1,000 °C (e.g., Lee et al. 1997). More recently, mounting evidence for retention of Pb in monazite at higher temperatures has been provided from experimental and field studies (e.g., Montel et al. 2000; Cherniak et al. 2000), and our data support this hypothesis.

Variation of residence times between sites

The long inferred residence times of anatectic magmas are not found at Mazarrón, where SHRIMP data indicate that anatexis and magma eruption were almost contemporaneous, and occurred when anatexis was taking place below El Joyazo. In the case that this difference in residence times between the two localities is real, and not an artefact related to sampling, an explanation is required.

It has been shown that the restitic enclaves record anatexis at different pressures at the two sites: c. 7 kbar at El Joyazo, and < 4.5 kbar at Mazarrón. This indicates that anatexis beneath El Joyazo took place at least 10 km deeper in the crust. The volumes of erupted volcanics are also very different: c. 1 km^2 of outcrop al El Joyazo vs. > 100 km^2 at Mazarrón. Thus, we may envisage that the anatectic magmas produced at Mazarrón, located at a relatively shallow level, could find easier and more rapid access to the surface through fractures in the more brittle crust. Conversely at El Joyazo, where partial melting was located almost at the base of the crust (Cesare and Gómez-Pugnaire 2001), the more ductile setting prevented immediate escape of the anatectic melts by upwelling towards the surface.

The Messinian age of eruption of the deep crustal melts of El Joyazo falls notably at the beginning of an important phase of uplift recorded in the eastern Iberian margin at the Messinian-Pliocene boundary (Janssen et al. 1993). This regional uplift may have favoured the uprise of the anatectic magmas of El Joyazo, which would otherwise have crystallized at depth as enclave-rich, S-type granitoids.

Constraints on crustal melting in the Internal Betics

The zircon and monazite data obtained in this study and their comparison with other data on Miocene high-grade settings in the Internal Betics allow a refined overview of the crustal melting processes in the area. In Fig. 12, the P–T paths and time constraints for various areas of the Internal Betics, in which crustal melting has been suggested or demonstrated, are compared to those of the restitic enclaves of El Joyazo and Mazarrón. Two differences are apparent: 1) the various portions of the Betic crystalline basement show typical decompressional paths at temperatures rarely exceeding 700 °C, thereby suggesting very small degrees of melting. In contrast, the restitic enclaves in the high-K calc-alkaline volcanics

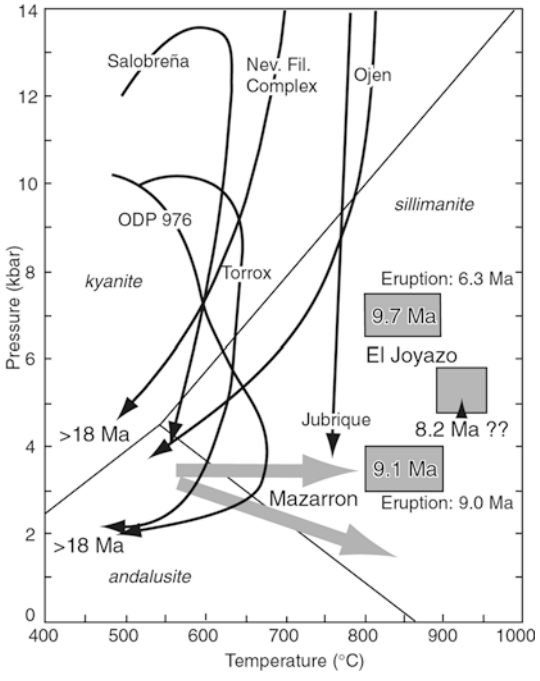

Fig. 12 Comparison of published P–T paths for various areas of the Internal Betic domain (*thin black arrows*, after Platt and Whitehouse 1999 and Gómez-Pugnaire et al. 1994), and thermobarometric estimates from the enclaves of El Joyazo and Mazarrón (*shaded boxes*). *Thick shaded arrows* outline the textural indications of andalusite replacement by sillimanite in the enclaves at Mazarrón. The larger P–T box for El Joyazo indicates conditions for the main anatectic event at 9.7 Ma, the smaller for the incongruent melting of biotite to hercynite (Cesare 2000)

indicate much higher temperatures (> 800 °C), and lack evidence of decompression. Additionally, the And-Sil transition observed in the enclaves of Mazarrón clearly indicates near-isobaric heating accompanying melting. 2) The possible crustal melting obtained by rapid decompression of the Betic crystalline basement occurred before c. 18 Ma, whereas enclaves attest to melting at c. 9 Ma with persistence of HT conditions to at least c. 6 Ma, the age of eruption of the dacite of El Joyazo.

From this dataset, we can conclude that silicic, S-type partial melts in the Internal Betics and in the Alborán Basin were produced in at least two different environments. An earlier LT setting synchronous with the main extensional exhumation phase in the early Miocene (see Platt et al. 2003), and a subsequent HT (or UHT) setting, of medium to low pressures, developed in the late Miocene. This latter scenario, responsible for the genesis of large volumes of S-type granitoids, was probably related to the presence of hot asthenosphere, and/or of mantle-derived magmas at the base of, or within, the thinned crust (e.g., De Larouziere et al. 1988).

The persistence of the thermal anomaly beneath the NVP and in the NE of the Alborán Basin can be evaluated on the basis of petrological, geochronological and geophysical data from the region. There is a general consensus that lithospheric thinning in the Internal Betics commenced in the early Miocene, at about 20 Ma. According to Turner et al. (1999) eruption of calc-alkaline crustal melts spans the interval 15–6 Ma, after which the lithosphere would have re-thickened and cooled. However, there are numerous indications in favour of a thermal anomaly remaining active in the southeastern margin of the Iberian Peninsula. These include the maximum values of surface heat flow measured in the Iberian Peninsula (> 80 mW m^{-2}; Fernandez et al. 1998), the anomalously thin lithosphere (< 60 km, Torne et al. 2000), and the presence an anomalously shallow, young oceanic crust in the east Alborán Sea (Polyak et al. 1996). Moreover, a low velocity anomaly at shallow depth (40–60 km) indicates the presence of hot asthenospheric mantle (Calvert et al. 2000). Further evidence for a thermal anomaly comes from data on the lower crust (Carbonell et al. 1998; Pous et al. 1999), the low seismic velocity and high electrical conductivity of which have been explained by the presence of partially molten rocks at depth (Zappone et al. 2000). These data suggest not only that favourable conditions for crustal melting at depth are possible, but also that melts are actually present in the lower crust.

Therefore, in keeping with the predictions of the numerical models of Arnold et al. (2001) we infer that the high thermal regime allowing crustal melting beneath the Internal Betics started at c. 18 Ma and is still active. This thermal high may have persisted continuously up to the present in the NVP and NE Alborán Basin, with possibly an additional heating pulse during the uplift phase at the Miocene-Pliocene boundary (Janssen et al. 1993). From this perspective, melt residence times much longer than 3 m.y. are possible. An alternative hypothesis is that the Miocene-Pliocene uplift recorded from surface data has a more important role, and testifies for deeper heating processes leading to crustal melting. From this point of view, the extensive crustal melting at c. 9 Ma, and the further melting episode at c. 8 Ma might result from the initial development of this phase of lithospheric thinning. We have no means of establishing which of these models is more sound, and additional detailed geochronological work is required.

Crustal melting and high-K calc-alkaline magmatism in the NVP: a summary

Along with Vera and Mar Menor, the volcanic edifices of Mazarrón and El Joyazo are the most important evidence in the NVP for silicic to intermediate high-K calc-alkaline magmas produced primarily by crustal melting. They are geochemically, chronologically and geographically distinct from the voluminous calc-alkaline volcanics of the Cabo de Gata area (Fig. 1). The Cabo de Gata volcanics are also interpreted as being derived from anatectic crustal melts (Zeck et al. 1998; Zeck and Whitehouse 2002), but are composed predominantly of basaltic andesites and andesites (Benito et al. 1999). Thus, the studied rocks are most important for the understanding of crustal melting processes related to the genesis of S-type granites.

The present work adds one further constraint, i.e., timing, to the petrologic model proposed by Cesare and Gómez-Pugnaire (2001), in which crustal melting in the Internal Betics was discussed in terms of its physical conditions, extent, setting and causes. The study of the restitic enclaves in the high-K calc-alkaline volcanics indicates that crustal melting occurred approximately at the base of the crust, where temperatures of 850 ± 50 °C or higher were reached. The degree of partial melting was very high (up to 60%, Cesare et al. 1997), with production of peraluminous felsic rhyolitic melts, remnants of which are still preserved in the enclaves as melt inclusions. Melting occurred c. 10 m.y. after lithospheric thinning in the area (Zeck et al. 1992), and was not related to significant decompression. Instead, petrological evidence indicates that it was due to very rapid, possibly isobaric, heating.

As pointed out by Zeck (1970), the restitic enclaves in the dacites of El Joyazo could be the product of: a) a crustal melting event genetically and temporally related to the Neogene volcanism; or b) the remelting of a pre-existing migmatitic basement of unknown age. Our data are consistent with the first scenario. They indicate that partial melting of a metapelitic crust took place in the late Miocene, and is genetically related with the coeval (Mazarrón) or c. 3 m.y. younger (El Joyazo) dacitic volcanism. There is no evidence that the graphitic source rocks had undergone migmatisation prior to c. 9 Ma. It is also unlikely that the source rocks were already

metamorphosed at upper amphibolite facies conditions before the onset of partial melting, as proposed by Zeck and Williams (2002). If the source rocks had been upper amphibolite facies metapelites or migmatites, a record of this high-grade metamorphism should be expected in the inherited zircon population. Such a signature is not documented by inherited zircon cores from the El Joyazo lava and enclave (Zeck and Williams 2002). Additionally, as discussed by Cesare and Maineri (1999), the presence of primary melt inclusions within all minerals of the enclaves, and the evidence for a finely spaced relict layering, make the hypothesis more likely that the source rocks were low-to medium grade graphitic metapelites, rapidly melted under disequilibrium conditions. The ubiquitous occurrence of graphite in both lavas and restites, and in the basement schists of the basal nappe sections, and its virtual absence in the metapelites of the cover sequences (Fallot et al. 1960; Egeler and Simon 1969), suggest that the source rocks are the graphite-bearing metapelites of the basement of the Betic-Alborán Domain.

Conclusions

Combined microstructural and U–Th–Pb SHRIMP analysis of zircon and monazite from enclaves of Mazarrón and El Joyazo have allowed dating of overgrowths which formed in the presence of a melt phase. We interpret such growth episodes as records of partial melting under HT, granulite-facies conditions. The partial melting of graphitic metapelites, which produced S-type leucogranitic magmas, is the main evidence for crustal anatexis in the Betic-Alborán Domain.

Ages obtained from zircon and monazite consistently overlap, and indicate that anatexis took place in the Tortonian, at c. 9.1 Ma at Mazarrón, and c. 9.7 Ma at El Joyazo. At El Joyazo, some data are interpreted to suggest the existence of a further melting event at c. 8.1 Ma.

While anatexis and eruption of crustal melts appear to be synchronous at Mazarrón, crustal melting is significantly older (>3 m.y.) at El Joyazo, where eruption has been dated at c. 6.3 Ma. It follows that the crustal melts resided at depth for at least 3 m.y.

The different residence times observed in the two locations can be related to the different depths at which crustal melting occurred: fairly shallow (c. 15 km) at Mazarrón, and much deeper (c. 25 km) at El Joyazo. In the latter case, the greater depth, and the more ductile regime of the crust, may have favoured magma ponding for c. 3 m.y., after which eruption was triggered. We expect that a (large) part of the crustal melts did not find a way up toward the surface. Thus, granitic plutons should be fairly common in the deep crust of the NVP and Alborán Basin. The present-day high heat flow in the southeastern Iberian margin attests to a long-lasting thermal anomaly in the area. It also suggests that the deep crust beneath the NVP may still contain large volumes of partially melted crust. From this perspective, residence times of up to 10 m.y. would be possible, especially for silicic volcanics such as those recently discovered in the Alborán seafloor (Comas et al. 1999).

Acknowledgements Many thanks to M. Fernández, A.M. Fioretti, S. Meli, and S. Tommasini for discussions, and to A. Möller, M. Bröcker, S. Turner and I. Williams for their thoughtful reviews. We acknowledge funding from the Università di Padova (Progetti di Ricerca) and C.N.R. (Westmed Euromargins ESF Eurocore) to B.C. and from Project BTE-2000-1489 (MCT) and RNM-145 (JA) to M.T.G-P. D.R thanks the Electron Microscopy Unit at the Australian National University for access to the SEM facilities and the Institute of Advanced Studies for financial support.

References

Annen C, Sparks RSJ (2002) Effects of repetitive emplacement of basaltic intrusions on thermal evolution and melt generation in the crust. Earth Planet Sci Lett 203:937–955

Arnold J, Jacoby WR, Schmeling H, Schott B (2001) Continental collision and the dynamic and thermal evolution of the Variscan orogenic crust—numerical models. J Geodyn 31:273–291

Benito R, Lopez-Ruiz J, Cebriá JM, Hertogen J, Doblas M, Oyarzun R, Demaiffe D (1999) Sr and O isotope constraints on source and crustal contamination in the high-K calc-alkaline and shoshonitic Neogene volcanic rocks of SE Spain. Lithos 46:773–802

Calvert A, Sandvol E, Seber D, Barazangi M, Roecker S, Mourabit T, Vidal F, Alguacil G, Jabour N (2000) Geodynamic evolution of the lithosphere and upper mantle beneath the Alborán region of the western Mediterranean: Constraints from travel time tomography. J Geophys Res 105:10871–10898

Carbonell R, Sallarés V, Pous J, Dañobeitia JJ, Queralt P, Ledo JJ, García-Dueñas V (1998) A multidisciplinary geophysical study in the Betic chain (southern Iberian Peninsula). Tectonophysics 288:137–152

Cesare B (2000) Incongruent melting of biotite to spinel in a quartz-free restite at El Joyazo (SE Spain): Textures and reaction characterization. Contrib Mineral Petrol 139:273–284

Cesare B, Gómez-Pugnaire MT (2001) Crustal melting in the Alborán domain: constraints from the xenoliths of the Neogene Volcanic Province. Phys Chem Earth (A) 26:255–260

Cesare B, Gómez-Pugnaire MT, Sanchez-Navas A, Grobety B (2002) Andalusite-sillimanite replacement (Mazarrón, SE Spain): microstructural and TEM study. Am Mineral 87:433–444

Cesare B, Maineri C (1999) Fluid-present anatexis of metapelites at El Joyazo (SE Spain): constraints from raman spectroscopy of graphite. Contrib Mineral Petrol 135:41–52

Cesare B, Salvioli Mariani E, Venturelli G (1997) Crustal anatexis and melt segregation in the restitic xenoliths at El Hoyazo (SE Spain). Mineral Mag 61:15–27

Cesare B, Marchesi C, Hermann J, Gómez-Pugnaire MT (2003) Primary melt inclusions in andalusite from anatectic graphitic metapelites: Implications for the position of the Al_2SiO_5 triple point. Geology 31:573–576

Chakraborty S, Ganguly J (1991) Compositional zoning and cation diffusion in aluminosilicate garnets. In: Ganguly J (ed) Diffusion, atomic ordering and mass transport—selected problems in geochemistry. Advances in physical geochemistry, vol 8, Springer, Berlin Heidelberg New York, pp 120–170

Cherniak DJ, Watson BE, Harrison MT, Grove M (2000) Pb diffusion in monazite: a progress report on a combined RBS/SIMS study. Suppl, Eos Trans 41 p 25

Comas MC, Platt JP, Soto JI, and Watts AB (1999) The origin and tectonic history of the Alborán Basin: Insights from Leg 161. In: Zahn R, Comas MC, Klaus A (eds) Proceedings ODP, Scientific Results, 161, 555–579

Compston W, Williams IS, Kirschvink JL, Zhang Z, Ma G (1992) Zircon U-Pb ages for the Early Cambrian time-scale. J Geol Soc Lond 149:171–184
Copeland P, Parrish RR, Harrison TM (1988) Identification of inherited radiogenic Pb in monazite and its implications for U-Pb systematics. Nature 333:760–763
Davies GR, Halliday AN (1998) Development of the Long Valley rhyolitic magma system: Strontium and neodynium isotope evidence from glasses and individual phenocrysts. Geochim Cosmochim Acta 62:3561–3574
De Larouziere FD, Bolze J, Bordet P, Hernandez J, Montenat C, Ott d'Estevou P (1988) The betic segment of the lithospheric Trans-Alborán shear zone during the late Miocene. Tectonophysics 152:41–52
Egeler CG, Simon OJ (1969) Sur la tectonique de la Zone Bétique (Cordillères Bétiques, Espagne). Verhanndelingen der Koninklijke Nederlandse Akademie van Wetenshappen 25:1-90
Fallot P, Faure-Muret A, Fontboté JM, Sole-Sabaris L (1960) Estudios sobre las series de Sierra Nevada y de la llamada Mischungszone. Bol Inst Geol Min 71:347–557
Fernández M, Marzán I, Correia A, Ramalho E (1998) Heat flow, heat production and lithospheric thermal regime in the Iberian Peninsula. Tectonophysics 291, 29–53
Fernández-Soler JM (1996) El volcanismo calco-alcalino en el parque natural de Cabo de Gata-Níjar (Almería). Estudio Volcanológico y Petrológico. Sociedad Almeriense de Historia Natural. Monografías del Medio Natural 2:1-295
Gómez-Pugnaire MT, Franz G, López Sánchez-Vizcaíno V (1994) Retrograde formation of NaCl-scapolite in high-pressure metaevaporites from the Cordilleras Béticas (Spain), Contrib Mineral Petrol 116:448–461
Heath E, Turner SP, Macdonald R, Hawkesworth CJ, van Calsteren P (1998) Long magma residence times at an island arc volcano (Soufriere, St. Vincent) in the Lesser Antilles: evidence from 238 U–230 Th isochron dating. Earth Planet Sci Lett 160:4-63
Janssen ME, Torné M, Cloethingh S, Banda E (1993) Pliocene uplift of the eastern Iberian margin: inferences from quantitative modeling of the Valencia Through. Earth Planet Sci Lett 119:585–597
Keay S, Lister G, Buick I (2001) The timing of partial melting, Barrovian metamorphism and granite intrusion in the Naxos metamorphic core complex, Cyclades, Aegean Sea, Greece. Tectonophysics 342:275–312
Kretz R (1983) Symbols for rock-forming minerals. Am Mineral 68:277–279
Kriegsman LM, Hensen BJ (1998) Back reaction between restite and melt: Implications for geothermobarometry and pressure–temperature paths. Geology 26:1111–1114
Lee JKW, Williams IS, Ellis DJ (1997) Pb, U and Th diffusion in natural zircon. Nature 390:159–161
Lopez Ruiz J, Rodriguez Badiola E (1980) La region volcanica Neogena del sureste de Espana. Estud Geol 36:5–63
Ludwig KR (2000) Isoplot/Ex version 2.4. A geochronological toolkit for Microsoft Excel. Berkeley, Berkeley Geochr Centre Spec Pub: 56
Montel JM, Kornprobst J, Vielzeuf D (2000) Preservation of old U–Th–Pb ages in shielded monazite: example from the Beni Boussera Hercynian kinzingites (Morocco). J Metamorph Geol 18:335–342
Ossan A (1889) Beiträge zur Kenntnis der Eruptiv gesteine des Cabo de Gata (Prov. Almería). Z Dtsch Geol Ges 41:287–311
Nichols GT, Berry RF, Green DH (1992) Internally consistent gahnitic spinel-cordierite-garnet equilibria in the FMASHZn system: geothermobarometry and applications. Contrib Mineral Petrol 111:362–377
Parrish RR (1990) U-Pb dating of monazite and its application to geological problems. Can J Earth Sci 27:1431–1450
Platt J, Vissers RLM (1989) Extensional collapse of thickened continental lithosphere: a working hypothesis for the Alborán Sea and Gibraltar arc. Geology 17:540–543
Platt JP, Soto JI, Whitehouse MJ, Hurford AJ, Kelley SP (1998) Thermal evolution, rate of exhumation, and tectonic significance of metamorphic rocks from the floor of the Alborán extensional basin, western Mediterranean. Tectonics 17:671–689
Platt JP, Whitehouse MJ (1999) Early Miocene high-temperature metamorphism and rapid exhumation in the Betic Cordillera (Spain): evidence from U–Pb zircon ages. Earth Planet Sci Lett 171:591–605
Platt JP, Whitehouse MJ, Kelley SP, Carter A, Hollick L (2003) Simultaneous extensional exhumation across the Alborán Basin: Implications for the causes of late orogenic extension. Geology 31:251–254
Polyak BG, Fernàndez M, Khutorskoy MD, Soto JI, Basov IA, Comas MC, Khain VYe, Alonso B, Agapova GV, Mazurova IS, Negredo A, Tochitsky VO, Bogdanov NA, Banda E (1996) Heat flow in the Alborán Sea (the western Mediterranean) Tectonophysics 263:191–218
Pous J, Queralt P, Ledo JJ, Roca E (1999) A high electrical conductive zone at lower crustal depth beneath the Betic Chain (Spain). Earth Planet Sci Lett 167:35–45
Reid MR, Coath CD, Harrison TM, McKeegan KD (1997) Prolonged residence times for the youngest rhyolites associated with Long Valley Caldera: 230 Th-238 U ion microprobe dating of young zircons. Earth Planet Sci Lett 150:327–39
Rubatto D, Williams IS, Buick IS (2001) Zircon and monazite response to prograde metamorphism in the Reynolds Range, central Australia. Contrib Mineral Petrol 140:458–468
Teufel S, Heinrich W (1997) Partial resetting of the U-Pb isotope system in monazite through hydrothermal experiments: an SEM and U-Pb isotope study. Chem Geol 137:273–281
Torne M, Fernández M, Comas MC, Soto JI (2000) Lithospheric structure beneath the Alborán Basin: Results from 3D Gravity modelling and tectonic relevance. J Geoph Res 105:3209–3228
Turner SP, Platt JP, George RMM, Kelley SP, Pearson DG, Nowell GM (1999) Magmatism associated with orogenic collapse of the Betic-Alborán Domain, SE Spain. J Petrol 40: 1011–1036
Vavra G, Gebauer D, Schmidt R, Compston W (1996) Multiple zircon growth and recrystallization during polyphase Late Carboniferous to Triassic metamorphism in granulites of the Ivrea Zone (southern Alps): an ion microprobe (SHRIMP) study. Contrib Mineral Petrol 122:337–358
Vissers RLM, Platt JP, van der Wal D (1995) Late orogenic and compositional constraints on 'post orogenic' magmatism. Geology extension of the Betic Cordillera and the Alborán Domain: a lithospheric view. Tectonics 14:786–803
Williams IS (2001) Response of detrital zircon and monazite, and their U-Pb isotopic systems, to regional metamorphism and host-rock partial melting, Cooma Complex, southeastern Australia. Aust J Earth Sci 48:557–580
Williams IS, Buick IS, Cartwright I (1996) An extended episode of early Mesoproterozoic metamorphic fluid flow in the Reynolds Range, central Australia. J Metamorph Geol 14:29–47
Zappone A, Fernández M, García-Dueñas V, Burlini L (2000) Laboratory measurements of seismic P-wave velocities on rocks from the Betic chain (southern Iberian Peninsula). Tectonophysics 317:259–272
Zeck HP (1968) Anatectic origin and further petrogenesis of almandine-bearing biotite-cordierite-labradorite-dacite with many inclusions of restite and basaltoid material, Cerro de Hoyazo, SE Spain. PhD Thesis, Amsterdam
Zeck HP (1970) An erupted migmatite from Cerro de Hoyazo, SE Spain. Contrib Mineral Petrol 26:225–246
Zeck HP (1992) Restite-melt and mafic-felsic magma mingling in an S-type dacite, Cerro del Hoyazo, southeastern Spain. Trans R Soc Edinb: Earth Sci 83:139–144
Zeck HP (1996) Betic-Rif orogeny: subduction of Mesozoic Tethys lithosphere under eastward drifting Iberia, slab detachment shortly before 22 Ma, and subsequent uplift and extensional tectonics. Tectonophysics 254:1–16

Zeck HP, Kristensen AB, Williams IS (1998) Post-collisional volcanism in a sinking slab setting—crustal anatectic origin of pyroxene-andesite magma, Caldear Volcanic Group, Neogene Alborán volcanic Province, southeastern Spain. Lithos 45:499–522

Zeck HP, Monie P, Villa IM, Hansen BT (1992) Very high rates of cooling and uplift in the Alpine belt of the Betic Cordilleras, southern Spain. Geology 20:79–82

Zeck HP, Whitehouse MJ (2002) Pre-eruptional magmatic zircon, Neogene Alborán volcanic province, SE Spain. J Geol Soc Lond 159:343–346

Zeck HP, Williams I (2002) Inherited and magmatic zircon from Neogene Hoyazo cordierite dacite, SE Spain—Anatectic source rock provenance and magmatic evolution. J Petrol 43:1089–1104